Journal of the European Ceramic Society **17** (1997) 929–934

PII: S0955-2219(96)00120-3
0955-2219/97/$17.00

The *In Situ* Formation of Sialon Composite Phases

S. Bandyopadhyay

Central Glass & Ceramics Research Institute, Calcutta 700 032, India

(Received 6 March 1996; revised version received 20 June 1996; accepted 15 July 1996)

Abstract

The in situ *formation of four sialon composites alpha-beta, alpha-15R, beta-15R and beta-12H in part of the system Y–Si–Al–O–N was investigated. The densification behavior of the alpha-beta materials differs from that of those containing polytypes. The alpha-based materials exhibit a unique composite microstructure where elongated grains of beta or plates of polytypes are embedded in an equiaxed matrix of alpha-sialon. This is important for the development of the strength and toughness of hard alpha-sialon ceramics. The properties of the composite phases are compared to those of the corresponding monolithic materials. © 1997 Elsevier Science Limited.*

1 Introduction

Sialon ceramics are promising candidates for engineering applications because of their excellent mechanical, chemical and thermal properties. β-Sialon (β') is an extended solid solution in the Si–Al–O–N system[1–3] which is based on the β-Si_3N_4 structure. Another solid solution, α-sialon (α'), is isostructural to α-Si_3N_4 and exists in the M–Si–Al–O–N system (M commonly yttrium).[4–12] Other polytype sialon phases based on the AlN type wurtzite structure occur in the AlN-rich zone of the Si–Al–O–N system.[13,14] All these phases are compatible along the α'–β'-containing plane Si_3N_4–$AlN.Al_2O_3$–MN.3AlN. These individual sialon phases have different intrinsic properties and different grain morphologies.

In this study, an investigation was made of the in-situ formation of different combinations of the sialon phases in different proportions from compositions in the system Y–Si–Al–O–N. The sintering characteristics and microstructures of the above materials are studied in detail. Some of the mechanical properties of the composite phases are compared with those of the single phases.

2 Experimental

β-Sialon with a low level of substitution (z up to 0·5) is difficult to sinter without additive.[15] A series of compositions (nos 1 to 7) was taken in this study along a line parallel to Si_3N_4–Y_2O_3.9AlN which originates from a β' composition corresponding to a z-value of 0·3 in the general formula $Si_{6-z}Al_zO_zN_{8-z}$ (Table 1). Two more compositions were taken by shifting the compositions nos 3 and 5 towards higher $AlN.Al_2O_3$ content where Y_2O_3 content is kept constant (nos 8 and 9, respectively). These two latter compositions correspond to the region containing β' and polytypes in the basic plane Si-Al–O–N. The starting powders were attrition milled with Si_3N_4 balls in an isopropanol medium, dried, sieved and pressed under an isostatic pressure of 630 MPa into green shapes. The green billets were fired under 1 MPa nitrogen gas pressure in an electrical resistance furnace. The phases were analyzed by XRD using Cu $K\alpha$ radiation. The samples were finished up to 1 μm and 6 μm for SEM and bending strength measurements respectively. The modulus of rupture was measured by using a four-point bending fixture with a span of 23 to 7 mm and with a cross-head speed of 0.01 mm/minute. Hardness was obtained by a Vickers diamond indentor using 10 kg load and the fracture toughness (K_{IC}) was estimated from the crack diagonals under indentation.[16]

3 Results and Discussion

The compositions are fired in a temperature range of 1500 to 1900°C. Above 1600–1650°C, no starting materials could be traced after 2 h firing. The ultimate phases are given in Table 1. All the compositions excepting nos 1 and 5 produce composite sialon phases. A two-phase mixture of α'–β' was obtained from compositions nos 2–4 in which the amount of α' is estimated from XRD to be

Table 1. The starting compositions and the final phases of the investigated samples

Comp. no.	*Mole%*			*Ultimate phases*
	Si_3N_4	$AlN.Al_2O_3$	$YN.3AlN$	
1	95·74	3·19	1·06	β
2	93·92	3·87	2·21	α'–β'
3	89·82	5·39	4·79	α'–β'
4	84·97	7·19	7·84	α'–β'
5	79·14	9·35	11·51	α'
6	72·00	12·00	16·00	α'–21R
7	63.06	15·32	12·62	α'–21R
8	49·18	44·26	6·56	β'–15R
9	52·63	33·33	14·04	β'–12H

about 10, 40 and 90%, respectively, i.e. increasing with increasing Y_2O_3 and AlN in the starting composition. The compositions nos 6 and 7 are three-phase mixtures of α', 21R sialon polytype (21R, $SiAl_6O_2N_6$) and nitrogen melilite ($Y_2Si_3O_3N_4$) in the lower temperature region. The amount of both 21R and melilite is larger in composition (no. 7) with higher Y_2O_3 and AlN content. The melilite disappears at above 1730°C and 1860°C for compositions 6 and 7, respectively, and the product becomes a composite material based on α' with 21R. As estimated from XRD, the amount of 21R is nearly double in composition no. 7. The last two compositions (nos 8 and 9) produce two β-sialon based composites with two other different polytypes, 15R ($SiAl_4O_2N_4$) and 12H ($SiAl_5O_2N_5$). The amount of polytype in these products is comparable to that of composition no. 7. The β'-polytype phases are stable at a temperature of 1600°C onwards.

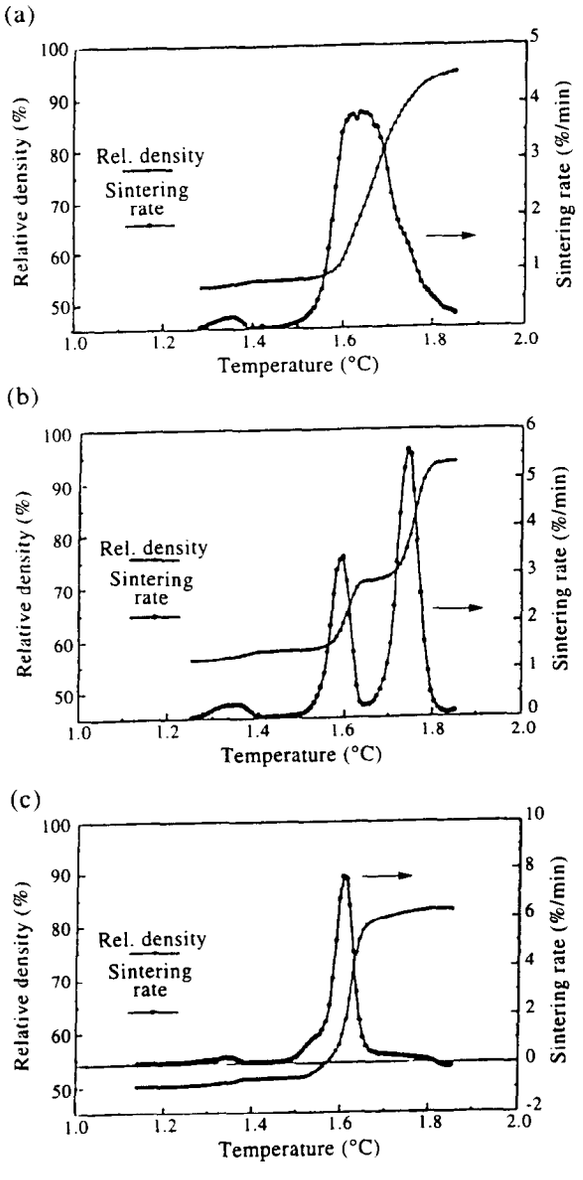

Fig. 1. The shrinkage behaviour and the derived densification rate of some of the compositions during heating up of the furnace: (a) α'-β'; (b) α'-polytype; (c) β'-polytype.

The dilatometric study was performed for all samples with a linear heating rate of 15°C/min under nitrogen gas at normal atmospheric pressure (Figs 1(a)–(c)). The typical shrinkage curves indicate the nature of sintering. The derived shrinkage rate when analyzed in association with the intermediate phases present reveals the reaction sequences during formation of the final product. The shrinkage starts for all the α'-based compositions at a temperature range of 1255 to 1295°C while that for β'-based compositions starts at a much lower temperature of below 1150°C. In all the compositions YAM ($Y_4Al_2O_9$) appears as the first transient phase, the amount of which is much larger in the case of β'-based compositions. In the first composition of α'–β' (high β' content) the measurable shrinkage starts above 1350°C. This may be due to the formation of an oxide melt in the system Y_2O_3–Al_2O_3–SiO_2, the SiO_2 being the oxide impurity of the starting Si_3N_4 powder (L1, Table 2). The liquid composition becomes an oxynitride (L2) above 1500°C when AlN and α–Si_3N_4 start dissolving into it. The dissolution of AlN is rapid and complete by 1570°C. The α' and β' start precipitating above 1600°C. The nature of the liquid phases in this case is similar to the pure α'-sialon compositions.[17] The next compositions of α'–β' materials involve a two-step sintering. The volume of oxide liquid is reduced because of the precipitation of the yttrium-containing crystalline phase YAG ($Y_3Al_5O_{12}$) which redissolves above around 1500°C into the oxynitride melt. The α'-polytype compositions involve a third intermediate step when the volume of the liquid is once again reduced following the precipitation of another yttrium-containing crystalline phase, nitrogen melilite ($Y_2Si_3O_3N_4$), in the temperature region of 1650 to 1700°C. The β'-based compositions exhibit a two-step sintering characteristic like α'–β' composites. Although 15R appears transiently around 1600°C, it does not affect the shrinkage curve. In all cases, the major

Table 2. Details of dilatometric study of the investigated compositions

Comp. no.	*Start of shrinkage (°C)*	*Intermediate steps*				*Transient phases*
		No. of steps	*Temperature range (°C)*	*Maximal sintering rate (°C)*	*(%/min)*	
2	1256	1	1355–1900	1654	2·3	L1,L2,Y1
3	1284	2	1300–1406	1376	0·3	L1,L2,Y1
			1468–1850	1628–1674	3·9	Y2
4	1238	2	1260–1414	1376	0·25	L1,L2,Y1
			1521–1850	1660	4·4	Y2
6	1287	3	1303–1462	1395	0·5	L1,L2,Y1
			1509–1670	1640	2·7	Y2,M
			1670–1800	1731	5·2	
7	1254	3	1277–1414	1353–1377	0·4	L1,L2,Y1
			1490–1660	1614	3·4	Y2,M
			1690–1800	1759	5·6	
8	1139	2	1322–1398	1368	0·2	L1,L2,Y1
			1498–1690	1621	7·9	Y2
9	1126	2	1311–1388	1355	0·5	L1,L2,Y1
			1547–1670	1631	13·0	Y2,15R

L1—oxide liquid, L2—oxynitride liquid, Y1—YAM, Y2—YAG, M—nitrogen melilite, 15R-sialon polytype.

amount of sintering takes place in the presence of the oxynitride liquid involving the second step of sintering. The most effective temperature region for densification of α'-based compositions is from 1600 to 1800°C while that for β'-based materials is strictly limited to below 1650°C. These latter compositions, however, sinter much faster than the α'-based compositions in the lower temperature region as indicated by the rate of sintering (Table 2), probably because of a larger volume of liquid.

The influence of sintering time on density under isothermal heating at 1750°C for the α'-based compositions is presented in Fig. 2. The densification in the case of α'–β' composites is faster than that of α'-polytype materials. The presence of melilite in the latter compositions brings the difference. The higher the melilite formation, the slower is the rate. In the polytype-containing compositions, melilite dissolves slowly into the liquid with time and the sintering proceeds. The overall densification, for all the materials in general, increases with soaking time up to 2 h. The final density values for all the compositions after 2 h sintering are given in Table 3. In the α'-polytype composites, the material containing less polytype densifies better. Amongst all, the α'–β' composite in about equal ratio shows the best densification. The β'-polytype composition undertaken in this study provides the advantage of low-temperature formation where the highest density value is achieved below 1650°C. A comparable density value for the similar material in the system La–Si–Al–O–N was achieved at 1900°C.[18]

Typical SEM micrographs using back-scattered electrons reconfirm the nature of phases present. The grain morphology and the distribution of the phases for α'–β' are shown in Figs 3(a)–(c). The white portion corresponds to a phase containing a heavy element and therefore, depending on the amount of yttrium present, different phases show

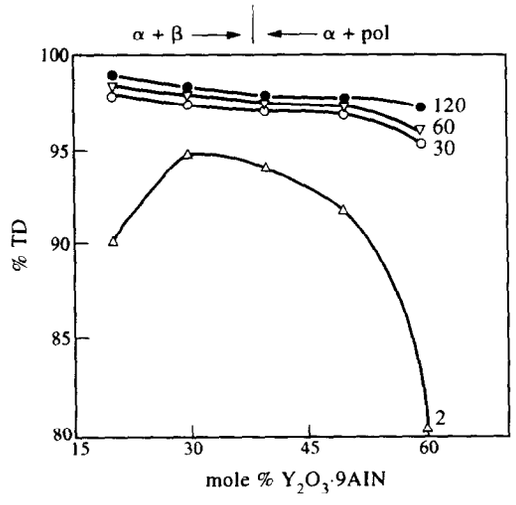

Fig. 2. The variation in densification with sintering time under an isothermal heating at 1750°C. The time in minutes is shown inside the graph.

Table 3. Weight loss and final density of the products fired for 2 h under 1 MPa nitrogen gas pressure; α'-21R(2) denotes composition with higher amount of polytype; density values in parentheses are at 1850°C

Phases	*Density (%TD)*				*Weight loss (%)*
	1650°C	*1700°C*	*1820°C*	*1900°C*	
α'–β'(2:3)	98·63	98·80	99·02	99·40	0·89–1·31
α'–β'(9:1)	97·91	98·01	98·16	98·26	0·76–1·38
α'–21R	96·48	97·59	97·99(98·01)	97·59	1·08–1·38
α'–21R(2)	94·59	94·11	94·89(97·10)	97·12	1·22–1·89
β'–15R	92·81	85·52	85·32	86·97	1·49–3·20
β'–12H	95·33	94·59	93·37	92·67	1·26–2·46

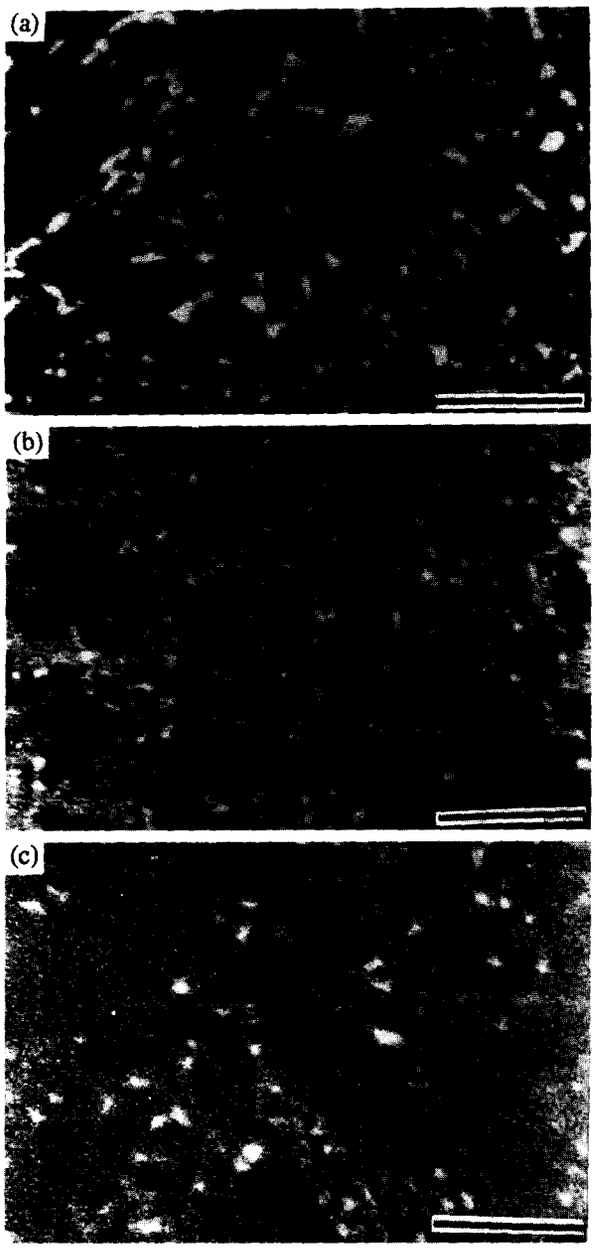

Fig. 3. SEM micrographs using back-scattered electrons of polished surface of α'-β' with a mutual ratio of: (a) 1:9; (b) 2:3; (c) 9:1; bar = 5 μm.

different levels of contrast. Dark crystals are β or β' as they contain only light elements and the white spots in all the compositions are the yttrium-rich glass. α' appears as a grey phase with an intermediate color between the two former phases. In general, it was seen that the elongated grains of β' are dispersed in an equiaxed matrix of α'. The size of the β' grains ranges between 3 and 7 μm with a maximum value up to 20 μm while the aspect ratio ranges between 3 and 5. The size of the α' is smaller around 3 μm. In the BSE micrograph of the α'-polytype material, the polytype appears as the dark crystals similar to the β' as they contain the same elements (Fig. 4(a)). The plasma-etched surfaces of this material reveal the long plate-like polytype grains (typically 7 to 10 μm) in an equiaxed α' matrix (Fig. 4(b)).

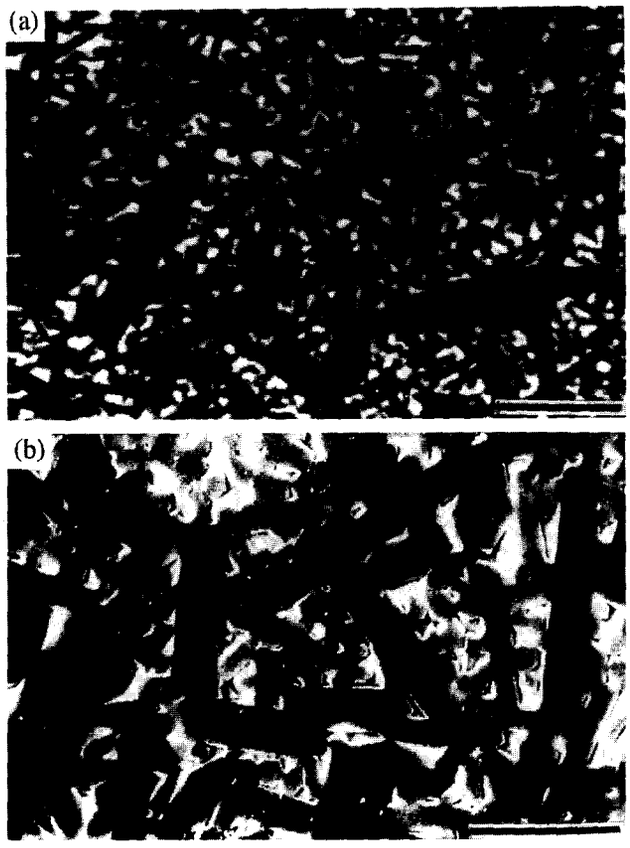

Fig. 4. SEM micrographs of α'-polytype (a) BSE image of polished surface, bar = 10 μm; (b) plasma-etched surface using a gas mixture of CF_4 and oxygen, bar = 5 μm.

The amount of the residual intergranular glass, appearing as white spots in the BSE micrographs, was measured by point counting and is presented as a function of starting composition (Fig. 5). Each point is a mean of four to six measurements where the deviations for the smaller values are ± 1% and for the larger ones ±3%. The remarkable feature is the drop in the remnant glass in α'-based materials. This may be attributed to the lesser availability of yttrium in these compositions to form the glass because of consumption of the cation to stabilize the α' structure. This point is important in minimizing the grain boundary glass for better high temperature properties without sacrificing the

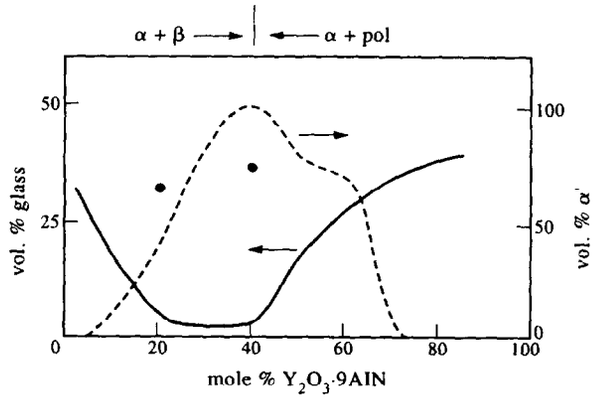

Fig. 5. The residual amorphous phase as a function of starting composition; solid line represents the α'-based compositions; filled circles are β'-polytype composition.

Table 4. Some of the mechanical properties of the fired products; α'-21R(2) denotes the composition containing higher amount of polytype

Phases	*Density (%TD)*	*MOR (MPa)*	K_{IC} *(MPa m$^{1/2}$)*	*Hardness (kg mm^{-2})*
α'-β'(2:3)	99·40	763	5·59	1760
α'-β'(9:1)	98·56	692	4·82	1990
α'-21R	98·01	441	4·37	1975
α'-21R(2)	97·10	389	4·25	1720
β'-15R	92·81	449	3·98	1476
β'-12H	95·33	486	4·40	1583
α'	98·13	464	4·66	2020
β'	98·82	745	4·72	1640

sinterability. The α'-β' shows minimum residual grain boundary. In comparison, α'-polytype is stabilized in a compositional zone where the Y_2O_3.9AlN content is much higher in the starting compositions.

Some of the mechanical properties of the composite materials are presented in Table 4. The introduction of β' in α' matrix increases the strength of the material sharply. The hardness of the composite ranges between that of monolithic α' and β' and increases with the α' content in the product. The fracture toughness is the best for α'-β' (about equal proportions) amongst all the materials in this study. However, no significant difference in any of the mechanical properties could be achieved when the polytypes are introduced in the α' matrix in place of β'. On the other hand, if the level of density achieved is kept in mind, it may be concluded that stronger material could be obtained from a β'-based composite material when the densification of the material is improved. Additionally, it may be economic due to the lower sintering temperature.

The retention of room-temperature strength of α'-β' is compared to that of monolithic α' and β' material (Table 5). The temperature dependence of this property is more or less similar for all the three materials. The post-sintering heat treated (at 1400°C for 24 h under 0·1 MPa nitrogen) α'-β' retains about three-quarters of its room-temperature strength at a temperature as high as 1350°C

4 Conclusions

Different composite sialon phases could be prepared from selected compositions in the plane Si_3N_4–Al_2O_3.AlN–YN.3AlN in the system Y–Si–Al–O–N. The densification behavior of these materials is influenced by the presence of both different transient crystalline phases as well as by the change in liquid compositions. The α'-β'-based materials require a higher temperature of formation

Table 5. Retention of room-temperature strength at higher temperatures; the values in parens are the standard deviations

Material	*Room-temperature strength (MPa)*	*Retention of RT strength (%)*		
		1200°C	*1300°C*	*1350°C*
β	745(80)	59·6		36·6
α'-β'(2:3)	763(26)	62·1	57·6	38·2
heat treated		72·7	73·8	76
α'	464(54)	70·7		40·7
heat treated		92·7		77·8

in comparison to the β' materials. The α'-β' sialon shows the best densification and the least amount of residual amorphous phase content at grain boundary. The elongated grains of β' contribute towards the improvement in strength and toughness while the amount of α' determines the hardness of the composite. The material exhibits excellent high-temperature strength retention. The β'-based material shows possibility of economic production for these kinds of composite ceramics.

Acknowledgements

The author is grateful to Prof. G. Petzow and Dr M. J. Hoffmann of Max Planck Institute, Stuttgart, Germany for their stimulating discussions. Thanks are due to the Director, Central Glass & Ceramic Research Institute, Calcutta, for his kind interest in the work.

References

1. Gauckler, L. J., Lukas, H. L. and Petzow, G., Contribution to the phase diagram Si_3N_4–AlN–Al_2O_3–SiO_2. *J. Am. Ceram. Soc.*, 1975, **58**, 346–347.
2. Jack, K. H., Review: Sialons and related nitrogen ceramics. *J. Mater. Sci.*, 1976, **11**, 1135–1158.
3. Bergman, B., Ekstrom, T. and Micski, A., The Si–Al–O–N system at temperatures of 1700–1775°C. *J. Eur. Ceram. Soc.*, 1991, **8**, 141–151.
4. Hampshire, S., Park, H. K., Thompson, D. P. and Jack, K. H., α-sialon ceramics. *Nature (London)*, 1978, **274**, 880–883.
5. Grand, G., Demit, J., Ruste, J. and Torre, J. P., Composition and stability of Y–Si–Al–O–N solid solutions based on α-Si_3N_4 structure. *J. Mater. Sci. Lett.*, 1979, **14**, 1749–1751.
6. Mitomo, M., Tanaka, H., Muramatsu, K. and Fujii, Y., The strength of α-sialon ceramics. *J. Mater. Sci. Lett.*, 1980, **15**, 2661–2662.
7. Huang, Z. K., Greil, P. and Petzow, G., Formation of α-Si_3N_4 solid solutions in the system Si_3N_4–AlN–Al_2O_3. *J. Am. Ceram. Soc.*, 1983, **66**, C96–97.
8. Stutz, D., Greil, P. and Petzow, G., Two-dimensional solid solution formation of Y-containing α-Si_3N_4. *J. Mater. Sci. Lett.*, 1986, **5**, 335–336.
9. Sun, W. Y., Tien, T. Y. and Yen, T. S., Subsolidus phase relationships in part of the system Si,Al,Y/N,O: The system Si_3N_4–AlN–YN–Al_2O_3. *J. Am. Ceram. Soc.*, 1991, **74**, 2753–2758.

10. Bartek, A., Ekstrom, T., Herbertsson, H. and Johansson, T., Yttrium α-sialon ceramics by hot isostatic pressing and post hot isostatic pressing. *J. Am. Ceram. Soc.*, 1992, **2**, 432–439.
11. Jasper, C. A. and Lewis, M. H., Novel α–β sialon ceramics. *4th. Int. Symp. on Ceramic Materials & Components for Engines*, ed. R. Carlsson, T. Johansson & L. Kahlman. Elsevier Science Publishers, London & New York, 1992, pp. 424–431.
12. Cao, G. Z., Metselaar, R. and Ziegler, G., Relation between composition and microstructure of sialons *J. Eur. Ceram. Soc.*, 1993, **11**, 115–122.
13. Thompson, D. P., Korgul, P. and Hendry, A., The structural characterization of sialon polytypoids. In *Progress in Nitrogen Ceramics*, ed. F. L., Riley. Martinus Nijhoff, The Hague, Netherlands, 1983, pp. 61–74.
14. Cannard, P. J., Ekstrom, T. and Tilley, R. J. D., The formation of phases in the AlN-rich corner of the Si–Al–O–N system. *J. Eur. Ceram. Soc.*, 1991, **8**, 375–382.
15. Bandyopadhyay, S. and Mukerji, J., Sintering and properties of sialons without externally added liquid phase. *J. Am. Ceram. Soc.*, 1987, **70**, C273–277.
16. Antis, G. R., Chantikul, P., Lawn, B. R. and Marshall, D. B., A critical evaluation of indentation techniques for measuring fracture toughness. *J. Am. Ceram. Soc.*, 1981, **64**, 533–538.
17. Nagel, A., Greil, P., and Petzow, G., Reaction sintering of yttrium-containing α-silicon nitride solid solution. *Revue de Chimie Minerale*, 1985, **t22**, 437–448.
18. Huang, H. R., Li, W. L., Feng, J. W., Huang, Z. K. and Yan, D. S., Si_3N_4–AlN polytypoid composites by GPS. *J. Eur. Ceram. Soc.*, 1991, **7**, 329–333.